

# Anion effects on ionogel formation in $N,N'$ -dialkylimidazolium-based ionic liquids <sup>☆</sup>

Millicent A. Firestone <sup>a,\*</sup>, Paul G. Rickert <sup>b</sup>, Sönke Seifert <sup>c</sup>, Mark L. Dietz <sup>b</sup>

<sup>a</sup> *Materials Science Division, Argonne National Laboratory, 9700 South Cass Avenue, Argonne, IL 60439, USA*

<sup>b</sup> *Chemistry Division, Argonne National Laboratory, Argonne, IL 60439, USA*

<sup>c</sup> *Advanced Photon Source Division, Argonne National Laboratory, Argonne, IL 60439, USA*

Received 4 May 2004; accepted 26 June 2004

Available online 29 July 2004

Dedicated to Professor T.J. Marks on the occasion of his 60th birthday

## Abstract

Addition of an appropriate concentration of water to either 1-decyl-3-methylimidazolium bromide or its nitrate analog is shown to trigger the self-assembly of the ionic liquid (IL) and the concomitant formation of gel (“ionogel”) phases adopting a rich variety of structural motifs. Infrared and <sup>1</sup>H nuclear magnetic resonance studies indicate that water addition disrupts hydrogen bonding between the imidazolium ring and the IL anion, and that gelation involves the partial replacement of these bonds with H-bonds between the anion and water. Using small angle X-ray scattering, the relationship of the water content and the nature of the IL anion to the mesoscopic structure of the ionogels has been determined. Of particular note is the observation that by adjustment of the ionogel composition (water content or anion), near-monodomain materials can be formed with either lamellar, 2-D hexagonal or 3-D cubic structures with tunable lattice dimensions.

Published by Elsevier B.V.

*Keywords:* Ionic liquid; Ionogel; Anion effects; Mesoscopic structure; SAXS

## 1. Introduction

Since the introduction of the first air- and water-stable ionic liquids (ILs) more than a decade ago [1], there has been increasing interest in their potential as substitutes for conventional organic solvents in a wide range of catalytic [2–4], electrochemical [5,6], and synthetic [7–10] applications. These compounds, which typically consist of

nitrogen- or phosphorus-containing organic salts characterized by sufficient asymmetry to inhibit their crystallization (and thus reduce their melting temperature to  $\leq 100$  °C), exhibit numerous properties that distinguish them from ordinary (i.e., molecular) organic solvents. For example, like classical molten salts, ionic liquids exist in a fully ionized state. As a result, they typically exhibit little or no vapor pressure [3]. In addition, they exhibit a wide liquidus range and electrochemical window [2,11]. Finally, and perhaps most importantly, ILs are extraordinarily tunable, with even minor changes in the structure of the anion or cation comprising the IL often having a substantial effect on its physicochemical properties [2].

This tunability is of obvious potential utility in the application of ILs in the design and synthesis of novel materials, and recently, there has been growing recognition of the possibilities offered by ILs in this area [12–19]. Of

<sup>☆</sup> The submitted manuscript has been created by the University of Chicago as Operator of Argonne National Laboratory (“Argonne”) under Contract No. W-31-109-ENG-38 with the US Department of Energy. The US Government retains for itself, and others acting on its behalf, a paid-up, non-exclusive, irrevocable worldwide license in said article to reproduce, prepare derivative works, distribute copies to the public, and perform publicly and display publicly, by or on behalf of the Government.

\* Corresponding author. Tel.: +630-252-8298; fax: +630-252-9151.

E-mail address: [firestone@anl.gov](mailto:firestone@anl.gov) (M.A. Firestone).

particular interest has been the use of ILs as templates in the fabrication of micro- and mesoporous inorganic and hybrid organic–inorganic materials. Adams et al. [12], for example, noting the surfactant-like nature of long-chain dialkylimidazolium salts, examined the use of 1-alkyl-3-methylimidazolium halides ( $[C_n\text{mim}^+][X^-]$ , with  $n=6-18$  and  $X^- = \text{Br}^-$  or  $\text{Cl}^-$ ) as replacements for the alkyltrimethylammonium salts normally employed as templates in the preparation of MCM molecular sieves. As is the case in conventional routes to MCM synthesis using  $[C_n\text{NMe}_3]^+X^-$  templates, best results were obtained for the hexadecyl-substituted ILs (i.e.,  $n=16$ ). Interestingly, however, MCM-41 of acceptable quality could be prepared only from the chloride-based ILs, suggesting a significant anion effect on template viability. More recently, Zhou et al. [15] have exploited hydrogen bond formation between an IL anion ( $\text{BF}_4^-$ ) and the silano group of silica gel and the  $\pi-\pi$  stack interactions between neighboring imidazolium rings to form a network of  $[C_4\text{mim}^+][\text{BF}_4^-]$  that served to template monolithic mesoporous silica. These same investigators have demonstrated [16] that highly ordered, monolithic “super-mesoporous” (pore size: 1–2 nm) lamellar silica can be produced using as a template the liquid crystalline (LC) phase of various long-chain (e.g.,  $n=16$ ) 1-alkyl-3-methylimidazolium chlorides. It remains unclear in either case if the results are anion-specific.

Our own work with ILs has concerned the preparation and characterization of liquid crystalline  $[C_n\text{mim}^+][X^-]$  “ionogels”, physical gels comprising mesoscopically ordered assemblies of relatively short-chain ( $n=10$ ) 1-alkyl-3-methylimidazolium salts. Recent work in our laboratory has shown, for example, that the addition of an appropriate concentration of water to 1-decyl-3-methylimidazolium bromide results in its spontaneous self-organization and the formation of a LC gel, thus demonstrating that ionogel formation requires neither the functionalization of the IL [20] nor the addition of an exotic mesogen [21] or organogelator [22]. As part of our ongoing efforts to exploit soft matter in the design and preparation of new materials [23,24] and, in particular, as a first step in an examination of the utility of ionogels as templates for the synthesis of mesoporous inorganic materials, we have undertaken an investigation of the origins of ionogel formation and of the relationship of the nature of the IL anion to the mesoscopic structure of ionogels. In this report, we describe our initial findings.

## 2. Experimental

### 2.1. Materials

#### 2.1.1. Ionic liquid synthesis

The ionic liquid 1-decyl-3-methylimidazolium bromide was synthesized and purified according to the pub-

lished procedures [25], characterized by  $^1\text{H}$  and  $^{13}\text{C}$  NMR, dried in vacuo at 80 °C, and stored in a desiccator until use. The corresponding nitrate was synthesized by a metathesis reaction involving treatment of an aqueous solution of  $[C_{10}\text{mim}^+][\text{Br}^-]$  with silver nitrate. The accumulated solids (AgBr) were removed by filtration and the IL recovered by evaporation of the water. Tests of the recovered IL showed no additional precipitate formation upon addition of  $\text{AgNO}_3$  solution. (It is important to note that this does not imply the complete absence of bromide ion, as the minimum achievable level of bromide contamination is dictated by the solubility product constant of AgBr in water,  $5.2 \times 10^{-13}$  [26]. Ion chromatographic determination of the bromide content of the  $[C_{10}\text{mim}^+][\text{NO}_3^-]$ , however, showed it to be less than the limit of detection for the method, 0.05% (w/w).) Nanopure water was used in the preparation of all solutions. All other materials were A.C.S. reagent grade and were used as received.

#### 2.1.2. Ionogel preparation

Ionogels were prepared by combining weighed quantities of water and the desired ionic liquid. To ensure that the gels produced were homogeneous, repeated vigorous mixing was required. Gentle warming, by reducing the viscosity of the mixture, facilitated the homogenization in most instances.

### 2.2. Methods

#### 2.2.1. Infrared characterization

All IR spectra (64 scans;  $4\text{ cm}^{-1}$  resolution) were obtained using a Nicolet Nexus Model 870 infrared spectrometer with samples placed between ZnSe windows.

#### 2.2.2. NMR spectroscopy

NMR measurements were performed using a Varian Unity/INOVA system incorporating a 300 MHz magnet (Oxford) and a Nalorac Z-SPEC 5 mm broadband probe. The nature of the water–IL interactions leading to gelation was probed by examining the effect of water addition upon the chemical shift of the protons of the  $[C_{10}\text{mim}^+]$  cation for  $[C_{10}\text{mim}^+][X^-]$  ( $X = \text{Br}^-$  and  $\text{NO}_3^-$ ). In an initial series of experiments, increasing quantities of water were added to weighed samples of  $[C_{10}\text{mim}^+][\text{Br}^-]$  in a series of NMR tubes, and the mixtures repeatedly warmed and mixed in an effort to obtain uniform samples. For mixtures containing either low (approximately  $\leq 0.16$ ) or high ( $\geq 0.8$ ) ratios of water to IL, the sample viscosity was such that a homogeneous sample could eventually be obtained and satisfactory NMR spectra could be acquired. For intermediate water contents, however, this was not the case, and efforts to obtain spectra directly on the ionogels were eventually abandoned. Instead, a concentrated (1 M) solution of the IL in deuterated acetonitrile was pre-

pared and placed in an NMR tube. This solution was then titrated with water added using a metered pipette and the chemical shift of the  $[\text{C}_{10}\text{mim}^+]$  protons measured as a function of water concentration. The small amount of non-deuterated acetonitrile present in  $\text{CD}_3\text{CN}$  was used as the internal reference for the chemical shift determination. ( $\text{CH}_3\text{CN}$  has a pentuplet centered at 1.93 ppm.) Because the IL contains a trace of water even after prolonged oven drying, the total water content of samples containing low added-water-to-IL ratios was determined by integration of the NMR spectrum.

### 2.2.3. Small-angle X-ray scattering studies

Small-angle X-ray scattering studies (SAXS) were carried out on  $[\text{C}_{10}\text{mim}^+][\text{Br}^-]$  and  $[\text{C}_{10}\text{mim}^+][\text{NO}_3^-]$  ILs containing either 17% or 40% (w/w) water. Viscous samples (e.g.,  $[\text{C}_{10}\text{mim}^+][\text{Br}^-]$  containing 17% (w/w) water) were loaded from the melt and held in glass capillaries fashioned from Pasteur pipettes. Low viscosity samples (e.g.,  $[\text{C}_{10}\text{mim}^+][\text{NO}_3^-]$  containing 40% (w/w) water) were loaded into 1.5 mm quartz capillaries by a syringe. SAXS measurements were performed on an undulator beamline (12ID-C) of the advanced photon source (APS) at Argonne National Laboratory. The scattering profiles were recorded with either a MarCCD-165 detector (Mar USA, Evanston, IL), which features a circular, 165 mm diameter active area and  $2048 \times 2048$  pixel resolution or on a custom-built mosaic detector (gold) consisting of 9 CCD chips with an image area of  $15 \times 5$  cm and  $1536 \times 1536$  pixel resolution. The area detector images were corrected for background scattering of the glass and quartz capillaries by subtracting from the recorded images an area detector image of the respective capillaries with the same exposure time as the ionogel/IL (1–5 s for the MarCCD and 0.1–0.5 s for gold). The sample-to-detector distance was set such that the detecting range for momentum transfer was  $0.004 < q < 1.5 \text{ \AA}^{-1}$ . The collected scattering data were calibrated on the basis of the known positions of silver behenate powder Bragg reflections. All samples were measured within 2 days of preparation.

## 3. Results and discussion

### 3.1. Origins of ionogel formation

In a prior communication [13], we noted that the formation of an ionogel upon addition of water to  $[\text{C}_{10}\text{mim}^+][\text{Br}^-]$  likely involved the formation of an H-bonded network comprising water, bromide ion, and the imidazolium cation. Such network formation could serve to enhance the segregation of the hydrophobic and hydrophilic segments of  $[\text{C}_{10}\text{mim}^+]$ , thus leading to regions of confined water and ultimately, to physical

gelation. Detailed experimental evidence in support of this contention was not provided, however. In an effort to obtain such evidence, we have carried out both infrared and  $^1\text{H}$  NMR investigations directed at the elucidation of the nature of the interaction between water molecules and the IL leading to gel formation.

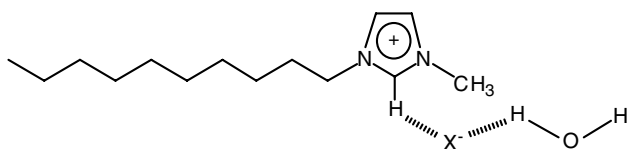
Consistent with the literature reports describing the infrared spectra of various  $[\text{C}_2\text{mim}^+][\text{X}^-]$  salts [27–29], the infrared spectrum of oven-dried  $[\text{C}_{10}\text{mim}^+][\text{Br}^-]$  exhibits a series of three prominent peaks at 2854, 2925, and  $2956 \text{ cm}^{-1}$  associated with aliphatic C–H stretching, a peak at  $3137 \text{ cm}^{-1}$  attributable to aromatic C–H stretching, and most notably, a peak at  $3058 \text{ cm}^{-1}$ , which has been attributed to C–H stretching for  $\text{C–H} \cdots \text{Br}^-$ . In addition, a series of weak peaks, referred to as “Sheppard effect bands” and arising from combinations of the three fundamental vibrational modes of  $\text{C–H} \cdots \text{Br}^-$  [29] are observed in the region between 2500 and  $2800 \text{ cm}^{-1}$ .

Upon uptake of water (ca. 1% w/w), a strong, broad band consistent with the O–H stretch for intermolecularly hydrogen-bonded water appears at  $3430 \text{ cm}^{-1}$ . At the same time, the peaks associated with the aromatic C–H stretch and the C–H stretch of the  $\text{C–H} \cdots \text{Br}^-$  moiety shift significantly (6 and  $16 \text{ cm}^{-1}$ , respectively) to higher wavenumbers. According to Pimentel and McClellan [30], the stretching mode of an A–H moiety is shifted to lower frequencies upon H-bond formation. The upward shift in the stretching frequency for  $\text{C–H} \cdots \text{Br}^-$  is thus consistent with disruption/diminution of H-bond formation between the imidazolium ring and the bromide ion upon addition of water. In contrast to these shifts, most of the bands for the  $[\text{C}_{10}\text{mim}^+][\text{Br}^-]$  remain essentially unchanged upon an increase in water content. The positions of the bands associated with aliphatic C–H stretching (2854, 2925 and  $2956 \text{ cm}^{-1}$ ), for example, are indistinguishable from those of the dried compound. The same can be said for the methylene scissoring and twisting bands ( $1466$  and  $1338 \text{ cm}^{-1}$ , respectively) and for the methyl symmetrical bending band ( $1378 \text{ cm}^{-1}$ ). Thus, as might be expected, the alkyl side-arms, unlike the imidazolium “headgroup”, are essentially unaffected by the presence of water.

Upon further addition of water and subsequent gelation, several additional changes in the spectrum become apparent. First, the position of the O–H stretching band falls to  $3421 \text{ cm}^{-1}$ , a shift of  $-9 \text{ cm}^{-1}$  relative to the corresponding peak in the spectrum of the fluid phase. At the same time, the position of the aromatic C–H stretch for  $\text{C–H} \cdots \text{Br}^-$  shifts upward by  $8 \text{ cm}^{-1}$  (for a total of  $24 \text{ cm}^{-1}$  versus the dried compound). In addition, the intensity of this band decreases significantly relative to that observed for the fluid phase. According to Pimentel and McClellan [30], the absorption coefficient of a stretching band will increase when a hydrogen bond forms. This decrease is thus indicative of a lessening of

H-bonding between C–H and  $\text{Br}^-$  upon addition of water/gelation. This is supported by the observation that the Sheppard effect bands of  $\text{C–H}\cdots\text{Br}^-$  weaken to the point of becoming barely discernible upon gel formation. In contrast, no effect on the peaks associated with aliphatic C–H stretching (methyl or methylene), bending (methyl), or scissoring (methylene) is evident.

According to LeGrange et al. [31] and Firestone et al. [32], the position of the asymmetric methylene stretching band is indicative of the degree of conformational order of the alkyl chains, with ordered, all-*trans* alkyl chains and disordered chains bearing *gauche* defects exhibiting peaks at 2918 and 2924  $\text{cm}^{-1}$ , respectively. This suggests that the  $\text{C}_{10}$  alkyl chains of  $[\text{C}_{10}\text{mim}^+][\text{Br}^-]$ , apparently disordered in the fluid state, remain so in the gel state. That is, the process of gelation has no discernible effect on the state of the alkyl chains of the imidazolium cation. Thus, gelation in this system manifests itself primarily by changes in the aromatic headgroup of the compound and the associated anion. Specifically, water addition appears to disrupt hydrogen bond formation between the imidazolium ring and the bromide ion, suggesting that gelation involves the partial replacement of these bonds with H-bonds between  $\text{Br}^-$  and water (I). (The existence of H-bonding between water and a halide ion in an IL is not, it should be noted, unprecedented. Lee et al. [33], for example, present X-ray crystallographic data indicating the presence of such interactions in various 1,3-dialkylbenzimidazolium salts, such as  $[(\text{C}_{12})_2\text{-Bim}^+][\text{Cl}^-]$ , and describe their significance in determining the structure of the compound.) That gel formation appears to arise from a balance between IL cation–anion and IL anion–water interactions is consistent with the recent studies by Cammarata et al. [34] of the state of water in  $[\text{C}_4\text{mim}^+][\text{Tf}_2\text{N}^-]$  (where  $\text{Tf}_2\text{N}^-$  represents the bis(trifluoromethyl)sulfonylimide anion) and related ILs, for which competition between the imidazolium cation and water for H-bonding with the IL anion was noted.



The results of  $^1\text{H}$  NMR studies in which the effect of water addition upon the observed chemical shift for the imidazolium ring protons of  $[\text{C}_{10}\text{mim}^+][\text{Br}^-]$  and the corresponding nitrate was examined are presented in Fig. 1. As can be seen, in both cases, addition of water to an acetonitrile solution of the IL results in a significant decrease in the chemical shift associated with the proton on C-2 (the carbon between the two nitrogen atoms in the imidazolium ring). Thus, this proton, which is initially

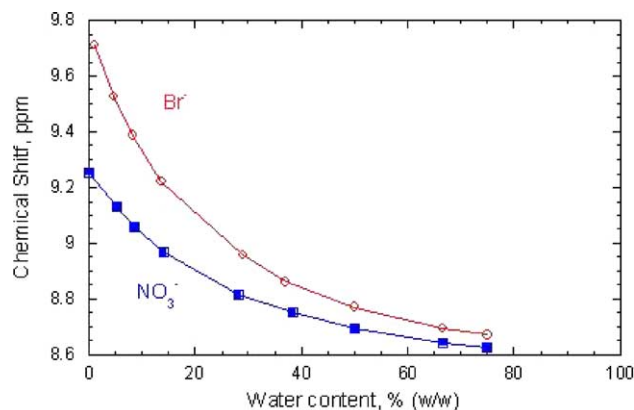


Fig. 1. Effect of water on the chemical shift of the C-2 proton of  $[\text{C}_{10}\text{mim}^+][\text{Br}^-]$  (open circles) and  $[\text{C}_{10}\text{mim}^+][\text{NO}_3^-]$  (solid squares) in  $\text{CD}_3\text{CN}$ .

significantly deshielded ( $\delta=9.712$  ppm and 9.254 ppm, respectively, for the bromide and nitrate ILs), gradually becomes less so as the water content of the solution rises. (Although the chemical shifts associated with all of the imidazolium ring protons are impacted by water addition, the effect is most pronounced for the C-2 proton, consistent with the reported greater acidity of this proton and the accompanying greater sensitivity of its chemical shift to changes in counteranion and solvent properties [35].) That the initial chemical shift is greater for the  $[\text{C}_{10}\text{mim}^+][\text{Br}^-]$  indicates that the interaction of bromide ion with the IL cation (in particular, with its C-2 proton) is stronger than for the nitrate anion, as expected given the greater basicity of  $\text{Br}^-$  [36]. The absence of any discontinuity in this plot at water:IL ratios corresponding to gelation is consistent with the view of gel formation suggested by the infrared results: that gelation results from the gradual establishment of a balance between IL cation–anion (specifically, C-2–H–anion) and anion–water interactions as the water concentration is increased.

Although we do not consider here the relationship between the molecular/ionic composition of ionogels/ILs and their macroscopic properties, it is interesting to note that  $[\text{C}_{10}\text{mim}^+][\text{Br}^-]$ , whose anion is apparently capable of stronger interaction with the IL cation, forms a robust (i.e., rigid) gel compared to the  $[\text{C}_{10}\text{mim}^+][\text{NO}_3^-]$ , which is a viscous liquid at room temperature. This is also supported by thermal analysis (differential scanning calorimetry, DSC), which reveals an endothermic transition,  $T_m$ , at 44.6  $^\circ\text{C}$  for the 16% (w/w)  $[\text{C}_{10}\text{mim}^+][\text{Br}^-]$  [13] versus 24.7  $^\circ\text{C}$  for  $[\text{C}_{10}\text{mim}^+][\text{NO}_3^-]$ .

### 3.2. Anion effects on ionogel/IL structure

The structural ordering of ILs on the mesoscopic length scale (nm– $\mu\text{m}$ ) makes them well suited for study by SAXS [13]. Moreover, this technique, unlike either electron microscopy or scanning probe methods, is

non-destructive and can probe the structure of soft materials without significantly perturbing them. Our prior SAXS studies of  $[\text{C}_{10}\text{mim}^+][\text{Br}^-]$  ionogels with water contents between 11% and 16% (w/w) showed that their mesoscopic structure is lamellar (i.e., a stacked, layered structure) (Fig. 2, LAM), as indicated by the appearance of two strong Bragg peaks at integral order spacing in the azimuthally averaged data [13]. The 2-D scattering pattern, however, displayed strong anisotropic scattering, with the scattered X-ray intensity predominantly directed along the equatorial axis, thus suggesting either directionally ordered lamellae or the onset of a structure with modulation (with hexagonal symmetry) of the lamellae, designated hexagonal modulated layer (HML) [37].

At a slightly higher water content than those employed previously, 17% (w/w), a structural transition to a higher order symmetry phase is observed (Fig. 3(a)). Specifically, the averaged 1-D data (Fig. 3(b)) display a single strong Bragg reflection and three weaker reflections (at  $q=0.218$  and  $0.378$ ,  $0.430$ , and  $0.572 \text{ \AA}^{-1}$ , respectively) that readily index to a hexagonal lattice ( $1:\sqrt{3}:2:\sqrt{7}$ ). From the position of the first-order peak, a  $d$ -spacing of  $28.8 \text{ \AA}$  can be determined. The 2-D scattering pattern shows that, as was the case at lower water contents, the scattered X-ray intensity is directed predominately in the equatorial direction. Nonetheless, the arcs show variations in intensity that make a six spot pattern readily apparent (Fig. 3(a)), indicating significant long-range, “single-crystal-like” ordering and suggesting a structural conversion to a hexagonally perforated layer mesophase (Fig. 2, HPL). Such mesophases have been reported for both surfactant-water systems [38,39] and diblock copolymers, and are often observed as intermediate structural states during the transition from a lamellar to a hexagonal phase associated with temperature jumps [40]. In di-

block copolymers, the HPL structure is characterized by penetration of layers of the minority component by the majority component, forming hexagonally arranged channels that serve to connect the layers [41].

The results presented here do not, it should be noted, suggest that the gel phase consists solely of an HPL structure under the experimental conditions. In fact, closer examination of Fig. 3(a) (making particular note of the higher order reflections in the 2-D images that are difficult to observe without saturating the first-order reflections) indicates that it possess features that may be consistent with the remnants of the characteristic 10-spot pattern of a gyroid (Ia3d) phase (Fig. 2, G), a phase characterized by a bicontinuous (interpenetrating) cubic network of two phases (i.e., water/anion and  $[\text{C}_{10}\text{mim}^+]$ ). The absence of Bragg reflections that index to ratios of  $\sqrt{6}$  and  $\sqrt{8}$  preclude the assignment of a true gyroid structure (G) to this phase, however. Thus, the structure of the gel at this water content is best described as HPL with some cubic character, perhaps indicative of conversion of the structure to a stable G phase at slightly higher water contents. It should also be noted that factors other than anion and water content, among them sample handling (e.g., loading), temperature, and sample history, could influence the mesophase structure.

When the water content of the  $\text{C}_{10}\text{mim}^+\text{Br}^-$  is increased sufficiently (to 40% (w/w)), the sample converts back to a low viscosity state and the 2-D scattering pattern becomes an isotropic ring, indicating a randomly oriented polydomain sample (Fig. 3(c)). Azimuthally averaging the 2-D data (Fig. 3(d)) yields two broad diffraction peaks at a ratio of  $1:\sqrt{3}$  ( $q=0.189$ ,  $0.320 \text{ \AA}^{-1}$ ), signaling conversion of the mesophase to a disordered hexagonal structure.

To determine the effect of a change in anion on the mesophase structure, analogous SAXS investigations

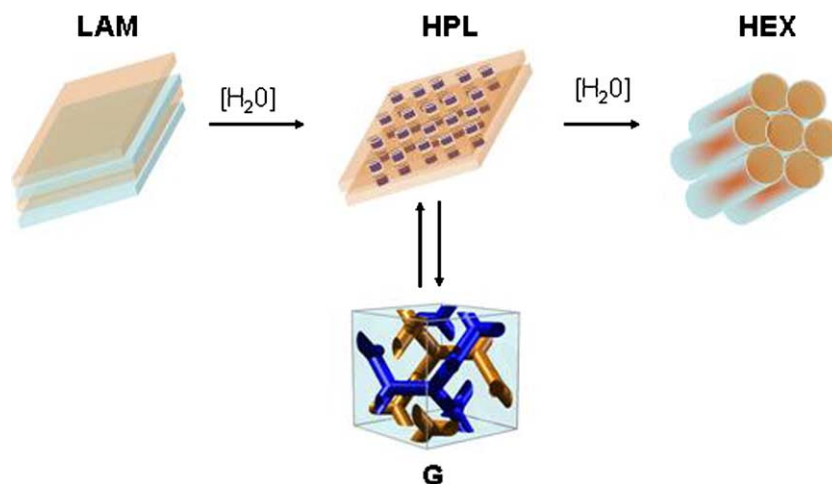


Fig. 2. Schematic illustrating the structural phases identified by SAXS on samples prepared with no additional water added  $[\text{C}_{10}\text{mim}^+][\text{Br}^-]$ : lamellar structure (LAM); 17% (w/w) added water  $[\text{C}_{10}\text{mim}^+][\text{Br}^-]$  and  $[\text{C}_{10}\text{mim}^+][\text{NO}_3^-]$ : hexagonal perforated layers (HPL) and gyroid structure (G); 40% (w/w) added water  $[\text{C}_{10}\text{mim}^+][\text{Br}^-]$  and  $[\text{C}_{10}\text{mim}^+][\text{NO}_3^-]$ : hexagonal structure (HEX).

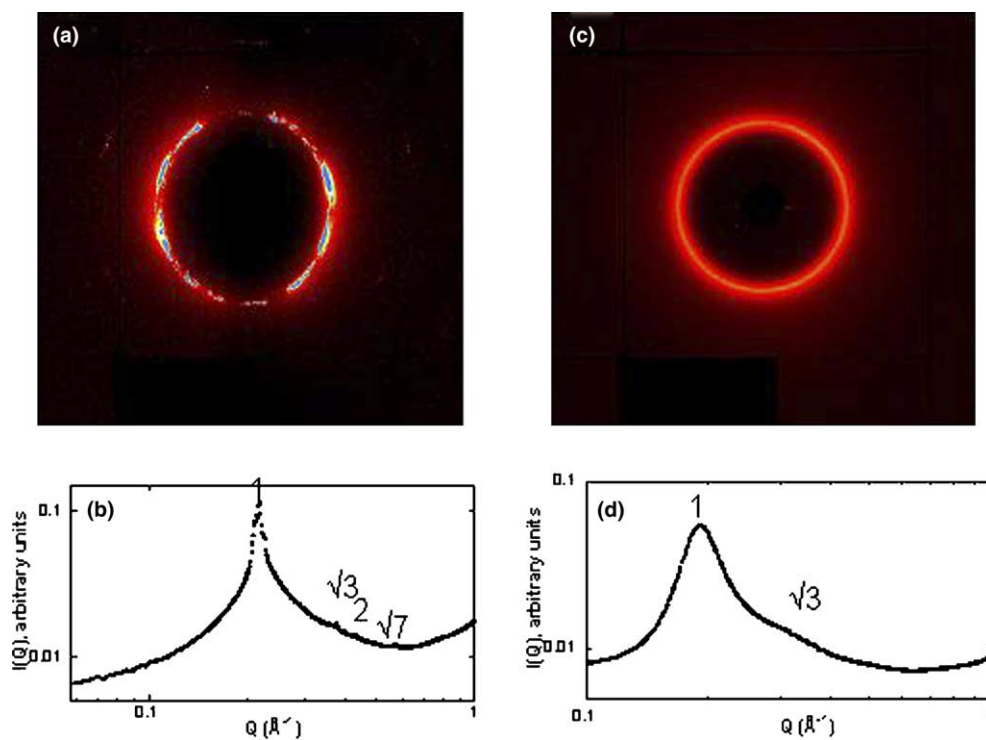


Fig. 3. (a) 2-D small-angle X-ray scattering pattern for a  $[\text{C}_{10}\text{mim}^+][\text{Br}^-]$  phase prepared with 17% (w/w) water added. (b) Azimuthally integrated scattering data presented in (a). (c) SAXS pattern from a  $[\text{C}_{10}\text{mim}^+][\text{Br}^-]$  phase prepared with 40% (w/w) water added. (d) Azimuthally integrated scattering data presented in (c).

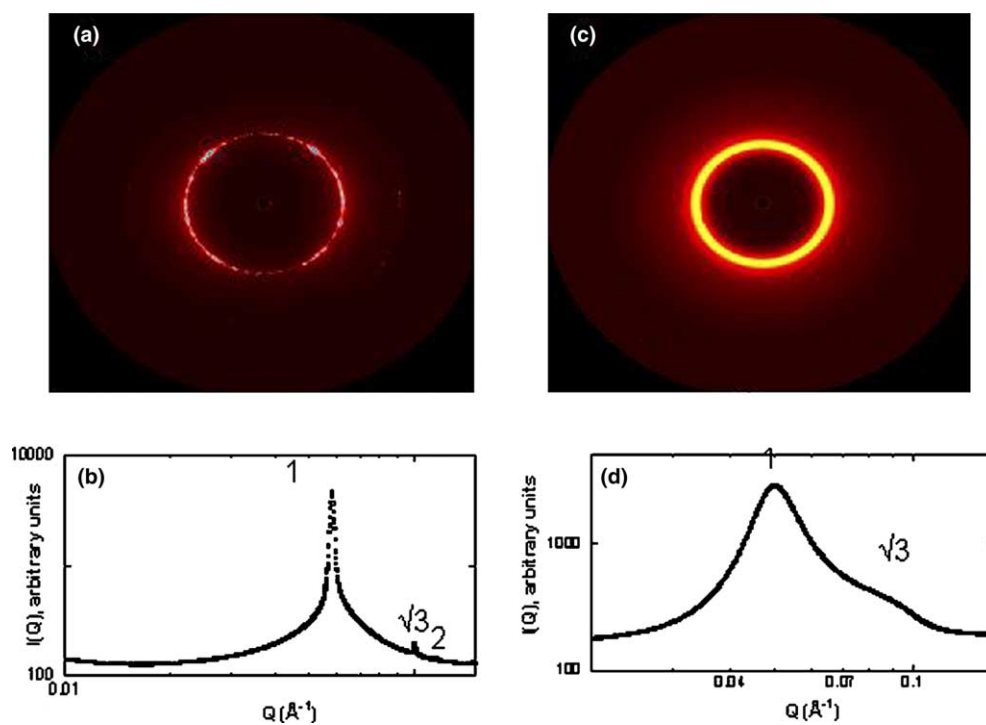


Fig. 4. (a) 2-D small-angle X-ray scattering pattern from a  $[\text{C}_{10}\text{mim}^+][\text{NO}_3^-]$  phase prepared with 16% (w/w) water added. (b) Azimuthally integrated scattering data presented in (a). (c) SAXS pattern from a  $[\text{C}_{10}\text{mim}^+][\text{NO}_3^-]$  phase prepared with 40% (w/w) water added. (d) Azimuthally integrated scattering data presented in (c).

of  $[C_{10}mim^+][NO_3^-]$  were carried out. The 1-D scattering curve for a nitrate ionogel containing 16% (w/w) water is presented in Fig. 4(b). Three diffraction peaks ( $q=0.058, 0.100, 0.116 \text{ \AA}^{-1}$ ), which can be indexed to a hexagonal structure (1: $\sqrt{3}$ :2), are observed. Interestingly, although the thermochemical radii of nitrate and bromide ions are comparable (1.96 and 1.88 Å, respectively) [42], the  $d$ -spacing for nitrate-based ionogel is 108.3 Å, more than three times that observed for the bromide-based gel (28.8 Å), implying that anion properties other than simply size (e.g., symmetry, bonding directionality) can exert a significant influence on the mesoscopic structure of ionogels. The 2-D SAXS pattern (Fig. 4(a)) at this water content is anisotropic, featuring a spot pattern similar to that observed for the corresponding bromide system, again suggestive of formation of a HPL type structure. In this case, however, preliminary data collected on a gel containing a lower water content (9% w/w; results not shown) suggest that 3-D cubic structures comprising a gyroid phase are formed (Fig. 2, G). Investigations on block copolymers have also demonstrated the epitaxial growth of oriented gyroid phases from hexagonal phases [43]. When the water concentration is increased to 40% (w/w), the structure of the nitrate ionogel, like that of the corresponding bromide, is found to convert to a disordered hexagonal structure, with the azimuthally averaged data exhibiting two broad reflections at 1: $\sqrt{3}$  (Fig. 4(d)). The appearance of both a diffuse isotropic ring in the 2-D image, as well as the breadth of the diffraction peaks in the 1-D curves, are indicative of a mesophase of poor spatial coherence.

#### 4. Conclusions

The results presented here, in addition to elucidating the origins of ionogel formation, clearly demonstrate that the mesophase structure (both symmetry and lattice dimensions) of IL-based gels can be “tuned” simply by careful selection of the anion and adjustment of the water concentration. Given that progress in the design of templated inorganic and hybrid organic–inorganic materials is dependent on the ability to control the structure of the underlying template, the ease with which the structure of  $[C_{10}mim^+][X^-]$  ionogels can be varied suggests that they may provide a versatile platform for the preparation of nano- and mesoporous materials. Work addressing these opportunities is now underway in this laboratory.

#### Acknowledgement

This work was performed under the auspices of the Office of Basic Energy Sciences, Division of Chemical (MLD, PGR) and Materials (MAF, SS) Sciences, US

Department of Energy, under contract number W-31-109-ENG-38. This manuscript is dedicated to Prof. Tobin Marks on the occasion of his 60th birthday.

#### References

- [1] J.S. Wilkes, M.J. Zaworotko, *J. Chem. Soc., Chem. Commun.* (1992) 965.
- [2] H. Olivier-Bourbigou, L. Magna, *J. Mol. Catal. A* 182 (2002) 419.
- [3] K.R. Seddon, *Kinet. Catal.* 37 (1996) 693.
- [4] D. Zhao, M. Wu, Y. Kou, E. Min, *Catal. Today* 74 (2002) 157.
- [5] J. Fuller, R.T. Carlin, R.A. Osteryoung, *J. Electrochem. Soc.* 144 (1997) 3881.
- [6] R.T. Carlin, J. Fuller, H.A. Frank, E.T. Seo, in: *Proceedings of the 12th Annual Battery Conference on Applications and Advances – 1997*, Institute of Electrical and Electronics Engineers, New York, 1997, pp. 261–266.
- [7] K.R. Seddon, *J. Chem. Technol. Biotechnol.* 68 (1997) 351.
- [8] J.D. Holbrey, K.R. Seddon, *Clean Prod. Process.* 1 (1999) 223.
- [9] M.J. Earle, K.R. Seddon, *Pure Appl. Chem.* 72 (2000) 1391.
- [10] A.E. Visser, W.M. Reichert, R.P. Swatloski, H.D. Willauer, J.G. Huddleston, R.D. Rogers, in: R.D. Rogers, K. Seddon (Eds.), *Ionic Liquids: Industrial Applications for Green Chemistry*, American Chemical Society, Washington, DC, 2002, pp. 289–308.
- [11] J.F. Brennecke, E.J. Maginn, *AIChE J.* 47 (2001) 2384.
- [12] C.J. Adams, A.E. Bradley, K.R. Seddon, *Aust. J. Chem.* 54 (2001) 679.
- [13] M.A. Firestone, J.A. Dzielawa, P. Zapol, L.A. Curtiss, S. Seifert, M.L. Dietz, *Langmuir* 18 (2002) 7258.
- [14] M.L. Dietz, J.A. Dzielawa, M.P. Jensen, M.A. Firestone, in: R.D. Rogers, K.R. Seddon (Eds.), *Ionic Liquids as Green Solvents: Progress and Prospects*, American Chemical Society, Washington, DC, 2003, pp. 526–543.
- [15] Y. Zhou, J.H. Schattka, M. Antonietti, *Nano Lett.* 4 (2004) 477.
- [16] Y. Zhou, M. Antonietti, *Chem. Mater.* 16 (2004) 544.
- [17] T. Nakashima, N. Kimizuka, *J. Am. Chem. Soc.* 125 (2003) 6386.
- [18] M. Yoshio, T. Mukai, H. Ohno, T. Kato, *J. Am. Chem. Soc.* 126 (2004) 994.
- [19] B. Lee, H. Luo, C.Y. Yuan, J.S. Lin, S. Dai, *Chem. Commun.* (2004) 240.
- [20] N. Kimizuka, T. Nakashima, *Langmuir* 17 (2001) 6759.
- [21] M. Yoshio, T. Mukai, K. Kanie, M. Yoshizawa, H. Ohno, T. Kato, *Adv. Mater.* 14 (2002) 351.
- [22] A. Ikeda, K. Sonoda, M. Ayabe, S. Tamaru, T. Nakashima, N. Kimizuka, S. Shinkai, *Chem. Lett.* (2001) 1154.
- [23] M.A. Firestone, P. Thiyagarajan, D.M. Tiede, *Langmuir* 14 (1998) 4688.
- [24] M.A. Firestone, D.E. Williams, S. Seifert, R. Csencsits, *Nano Lett.* 1 (2001) 129.
- [25] J.G. Huddleston, H.D. Willauer, R.P. Swatloski, A.E. Visser, R.D. Rogers, *Chem. Commun.* (1998) 1765.
- [26] D.A. Skoog, D.M. West, *Fundamentals of Analytical Chemistry*, third ed., Holt, Rinehart, and Winston, New York, 1976.
- [27] A.K. Abdul-Sada, A.M. Greenway, P.B. Hitchcock, T.J. Mohammed, K.R. Seddon, J.A. Zora, *J. Chem. Soc., Chem. Commun.* (1986) 1753.
- [28] J. Fuller, R.T. Carlin, H.C. DeLong, D. Haworth, *J. Chem. Soc., Chem. Commun.* (1994) 299.
- [29] A. Elaiwi, P.B. Hitchcock, K.R. Seddon, N. Srinivasan, Y.-M. Tan, T. Welton, J.A. Zora, *J. Chem. Soc., Dalton Trans.* (1995) 3467.
- [30] G.C. Pimentel, A.L. McClellan, *The Hydrogen Bond*, W.H. Freeman, San Francisco, 1960.
- [31] J.D. LeGrange, J.L. Markham, C.R. Kurkjian, *Langmuir* 9 (1993) 1749.

- [32] M.A. Firestone, M.L. Shank, S.G. Sligar, P.W. Bohn, *J. Am. Chem. Soc.* 118 (1996) 9033.
- [33] K.M. Lee, C.K. Lee, I.J.B. Lin, *Chem. Commun.* (1997) 899.
- [34] L. Cammarata, S.G. Kazarian, P.A. Salter, T. Welton, *Phys. Chem. Chem. Phys.* 3 (2001) 5192.
- [35] A.D. Headley, N.M. Jackson, *J. Phys. Org. Chem.* 15 (2002) 52.
- [36] R. Shukla, T. Kida, B.D. Smith, *Org. Lett.* 2 (2000) 3099.
- [37] M.E. Vigild, K. Almdal, K. Mortensen, I.W. Hamley, J.P.A. Fairclough, A.J. Ryan, *Macromolecules* 31 (1998) 5702.
- [38] Y. Rancon, J. Charvolin, *J. Phys. Chem.* 92 (1988) 2646.
- [39] M. Imai, A. Kawaguchi, A. Sacki, K. Nakaye, T. Kato, K. Ito, Y. Amemiya, *Phys. Rev. E* 62 (2000) 6865.
- [40] S. Qi, Z.G. Wang, *Phys. Rev. E* 55 (1997) 1682.
- [41] C.-Y. Wang, T.R. Lodge, *Macromolecules* 35 (2002) 6997.
- [42] B.A. Moyer, P.V. Bonnesen, in: A. Bianchi, K. Bowman-James, E. Garcia-Espana (Eds.), *Supramolecular Chemistry of Anions*, Wiley-VCH, New York, 1997, pp. 1–44.
- [43] J.-H. Ahn, W.-C. Zin, *Macromol. Res.* 11 (2003) 153.